

Systematic and efficient pseudomode method to simulate open quantum systems under a bosonic environment

L. K. Zhou,¹ G. R. Jin,^{2,*} and W. Yang^{1,†}

¹*Beijing Computational Science Research Center, Beijing 100193, China*

²*Key Laboratory of Optical Field Manipulation of Zhejiang Province and Physics Department of Zhejiang Sci-Tech University, Hangzhou 310018, China*



(Received 12 May 2024; revised 12 July 2024; accepted 5 August 2024; published 19 August 2024)

Using the pseudomode model to simulate open quantum systems is important in quantum physics. Here we report a systematic and efficient pseudomode model based on dissipative, noninteracting harmonic oscillators, capable of accurately simulating any type of environmental spectrum. The dynamical evolution is reduced to a Lindblad master equation with only one dissipation term. A simple procedure to determine the parameters of the pseudomodes is proposed. We evaluate its accuracy by some spin-boson models under different environmental spectra. Our findings consistently exhibit high accuracy. Finally, we extend this pseudomode method to larger systems with more complicated interactions. Our method may have potential applications in quantum information.

DOI: [10.1103/PhysRevA.110.022221](https://doi.org/10.1103/PhysRevA.110.022221)

I. INTRODUCTION

In quantum physics, the system of interest most often interacts with its surrounding environment, i.e., an open quantum system (OQS). A typical description of the OQS dynamics is the reduced density operator, obtained by tracing out the environmental degrees of freedom [1,2]. To solve the dynamical evolution, a well-known treatment is the Born-Markov approximation, which requires weak system-environment coupling and a large separation between system and environment timescales. Under the Born-Markov approximation, the reduced dynamics of the OQS can be described by a master equation [3,4]. However, in many practical scenarios such as solid state physics, hybrid systems, quantum biology and quantum optics, the Born-Markov approximation is no longer suitable, leading to distinct non-Markovian behavior [5–8]. Therefore, it is crucial to develop an accurate and efficient description or simulation of a non-Markovian OQS.

A wide range of physical environments can be described by Gaussian baths (such as those consisting of bosonic and fermionic degrees of freedom at thermal equilibrium) linearly coupled to the system. In this case, all effects of the environment on the system are fully characterized by the second-order correlation functions (hereafter referred to as COFs) of the environmental operators coupled to the system. To simulate the OQS, various numerical methods have been proposed, including the stochastic Schrödinger equations (SSE) theory [9–14], the quasiadiabatic propagator path integral [15–19], the time-dependent density-matrix renormalization group [20–22] or matrix product states [23–27], the non-Markovian cascaded

networks [28–31], and the hierarchical equations of motion (HEOM) theory [32–41].

The pseudomode method [42–49] provides an alternative route for the numerical study of such nontrivial open-system problems. The key idea of this method is to replace the original environment by some discrete dissipative quantum harmonic oscillators (known as pseudomodes). These pseudomodes are designed such that their COFs exactly reproduce the COFs of the original environment. The evolution of the system + pseudomodes can be described by a Lindblad master equation, which provides the simplest description for the OQS.

Regarding the pseudomode methods, a practical issue is how to design the pseudomode model to make its COFs exactly match any given COFs of the original environment. One strategy is to use some exponential functions to fit the original environmental COFs and then determine suitable pseudomode parameters to make their COFs match these exponential functions [44,46,47]. Recently, a powerful stochastic pseudomode model based on a “quantum-classical” decomposition has been proposed [48]. The idea is to simulate the “classical” part of the environmental COF by introducing some classical stochastic processes and reproduce the “quantum” part of the COF by the pseudomodes. Among these pseudomode methods, achieving high accuracy requires more pseudomodes or more stochastic processes, which significantly increase the computational cost. It is essential to develop a systematic approach that minimizes the computational costs while maintaining high accuracy in simulating the OQS. Additionally, the parameters of the pseudomodes should be determined using a simple method.

In this research, we present an efficient pseudomode model to accurately simulate the OQS. Our model utilizes a small number of noninteracting dissipative pseudomodes, eliminating the need for pseudomode-pseudomode interactions or

*Contact author: grjin@zstu.edu.cn

†Contact author: wenyang@csr.ac.cn

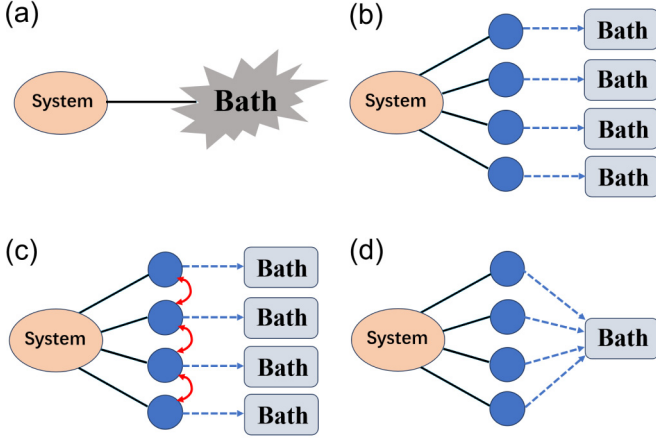


FIG. 1. (a) The original open quantum system problem. The system couples to a non-Markovian boson bath. (b) A pseudomode model based on local dissipated harmonic oscillators. The system couples with some pseudomode harmonic oscillators (blue solid circles) locally dissipated in the respective Markovian baths. (c) A pseudomode model based on locally dissipated harmonic oscillators with an oscillator-oscillator interaction chain. The system couples with some self-interacting pseudomode harmonic oscillators, and the oscillators are also locally dissipated in the respective Markovian baths. (d) A pseudomode model based on collective dissipated harmonic oscillators. The system couples with some pseudomode harmonic oscillators, and the oscillators are collectively dissipated in a single Markovian bath.

stochastic processes. The system's dynamical evolution is governed by a Lindblad master equation with a single dissipation term. Given an arbitrary environmental spectrum, the parameters of these pseudomodes can be determined through straightforward procedures. Notably, the frequencies and dissipation rates of these pseudomodes can be directly determined by a simple equation group, irrespective of the number of pseudomodes being employed. We evaluate our method's accuracy using two exactly solvable spin-boson models under different environmental spectrums. Additionally, we examine a more complicated spin-boson model and validate our approach by comparing it with the HEOM method. Our findings consistently exhibit high accuracy. We also extend our pseudomode model to larger systems with more intricate interactions.

II. OPEN QUANTUM SYSTEM PROBLEM

As illustrated in Fig. 1(a), we consider a system coupling to a boson environment or bath. The total Hamiltonian is given by

$$\hat{H}_{\text{tot}} = \hat{H}_s + \hat{H}_{\text{env}} + \hat{V}, \quad (1)$$

where \hat{H}_s , \hat{H}_{env} , and \hat{V} are the Hamiltonians of the system, the environment, and the interaction, respectively. The environmental Hamiltonian reads

$$\hat{H}_{\text{env}} = \sum_k \omega_k \hat{b}_k^\dagger \hat{b}_k, \quad (2)$$

where b_k is the k th boson mode's annihilation operator of the environment, with the characteristic frequency ω_k . We consider the interaction Hamiltonian

$$\hat{V} = \hat{S} \otimes \hat{B}, \quad (3)$$

where \hat{S} is the operator in the system's Hilbert space and $\hat{B} = \sum_k g_k \hat{b}_k + g_k^* \hat{b}_k^\dagger$ is the operator in the environment's Hilbert space.

We assume the initial state can be written as $\rho_s(0) \otimes \rho_B(0)$, where $\rho_s(0)$ and $\rho_B(0)$ are the initial states of the system and the environment, respectively. Meanwhile, we assume $\rho_B(0)$ is a thermal equilibrium state (a Gaussian state) at temperature T . The effects of the system-environment interaction are fully characterized by the COF, given by [1]

$$C(t) = \int_0^\infty d\omega J(\omega) \left[\coth\left(\frac{\omega}{2K_b T}\right) \cos(\omega t) - i \sin(\omega t) \right], \quad (4)$$

where $J(\omega) \equiv \sum_k |g_k|^2 \delta(\omega - \omega_k)$ is the spectral density function and K_b is the Boltzmann constant. The reduced density matrix of the system can be expressed in the interaction picture as [32–34,48]

$$\tilde{\rho}_s(t) = \mathcal{T} \exp \left\{ - \int_0^t d\tau_1 \tilde{S}(\tau_1)^\times \int_0^{\tau_1} d\tau_2 [C_R(\tau_1 - \tau_2) \tilde{S}(\tau_2)^\times + i C_I(\tau_1 - \tau_2) \tilde{S}(\tau_2)^o] \right\} \rho_s(0), \quad (5)$$

where $\tilde{S}(t) \equiv e^{i\hat{H}_s t} \hat{S} e^{-i\hat{H}_s t}$, $A^\times \hat{\rho} \equiv A \hat{\rho} - \hat{\rho} A$, $A^o \hat{\rho} \equiv A \hat{\rho} + \hat{\rho} A$, and C_R (C_I) is the real (imaginary) part of the COF. If the system's initial state $\rho_s(0)$ and the operator \hat{S} are given, $\tilde{\rho}_s(t)$ is fully dominated by the COF. The key task is to calculate the reduced density matrix $\tilde{\rho}_s(t)$ efficiently.

III. PSEUDOMODE MODEL

To calculate the reduced density matrix of the system, one choice is the HEOM method [32–41]. However, the HEOM method is complicated and its physical meaning is not intuitive. In recent years, it has been found that the original problem can be replaced by introducing some dissipated pseudomode harmonic oscillators with appropriate parameters. If the COF of the pseudomode model matches the original COF, the pseudomode model is equivalent to the original one.

Generally, the COF of pseudomode harmonic oscillators is a discrete sum of exponential functions, but the COF of the original model is usually nonexponential. Therefore, a common treatment is to fit the COF by a discrete set of exponential functions, which is similar to the HEOM method. Under the premise of ensuring accuracy and computation cost, we must use the least amount of exponential functions as possible. Because more exponential functions requires more pseudomode harmonic oscillators, which significantly enlarges the Hilbert space and hence increases the computation cost. Fortunately, the Prony method helps us use very few exponential functions to fit the COF $C(t) \approx \sum_j \lambda_j e^{\gamma_j t}$ with high accuracy, where the parameters λ_j and γ_j are generally complex numbers. If one considers the pseudomode model shown in Fig. 1(b), those λ_j values are limited within the field of real numbers

[44], which is unable to meet demand. Reference [46] proposed a pseudomode model involving an interaction chain of oscillator-oscillator [shown in Fig. 1(c)], which extended λ_j to the complex number field. However, determining the parameters of the pseudomodes to match the original COF is complicated and requires a difficult random sampling process.

In this work, we propose a simplified pseudomode model shown in Fig. 1(d). The system couples to M pseudomode harmonic oscillators, but the oscillators are collectively dissipated in a single Markovian bath, without any interaction of oscillator-oscillator. The total Hamiltonian of such a model is given by

$$\hat{H}_{\text{pse}} = \hat{H}_s + \hat{S} \otimes \hat{B} + \hat{H}_B, \quad (6)$$

with

$$\hat{B} = \sum_{j=1}^M \eta_j \hat{c}_j^\dagger + \eta_j^* \hat{c}_j \quad (7)$$

and

$$\begin{aligned} \hat{H}_B = & \sum_{j=1}^M \Omega_j \hat{c}_j^\dagger \hat{c}_j + \sum_k \omega_k \hat{b}_k^\dagger \hat{b}_k \\ & + \sum_k \sum_{j=1}^M g_{j,k} \hat{b}_k \hat{c}_j^\dagger + g_{j,k}^* \hat{b}_k^\dagger \hat{c}_j. \end{aligned} \quad (8)$$

Here, η_j denotes the interaction strength between the system and the j th harmonic oscillator, $g_{j,k} = \mu_j g_k$ denotes the coupling strength between the j th harmonic oscillator and the k th boson model of the bath (note that there is only one bath). For convenience, we consider a constant coupling strength g_k (i.e., the harmonic oscillators are dissipated in a Markovian bath) and we assume that the bath is initially in the vacuum state. We emphasize that the harmonic oscillators are characterized by Markovian dissipation, but the system is characterized by non-Markovian dissipation. In the following, we show that using few harmonic oscillators with collective Markovian dissipation can accurately simulate any non-Markovian environment.

If we view the system and the pseudomode harmonic oscillators as a whole, it undergoes dissipation within a Markovian bath, in which dynamical evolution is governed by the Lindblad master equation

$$\frac{\partial \rho_{\text{sc}}}{\partial t} = -i[\hat{H}, \rho_{\text{sc}}] + \mathcal{D} \left[\sum_{j=1}^M \mu_j \hat{c}_j \right] \rho_{\text{sc}}, \quad (9)$$

where

$$\hat{H} = \hat{H}_s + \sum_{j=1}^M \Omega_j \hat{c}_j^\dagger \hat{c}_j + \hat{S} \otimes \sum_{j=1}^M (\eta_j \hat{c}_j^\dagger + \eta_j^* \hat{c}_j) \quad (10)$$

and

$$\mathcal{D}[\hat{A}] \rho_{\text{sc}} \equiv \hat{A} \rho_{\text{sc}} \hat{A}^\dagger - \frac{\rho_{\text{sc}} \hat{A}^\dagger \hat{A} + \hat{A}^\dagger \hat{A} \rho_{\text{sc}}}{2}. \quad (11)$$

Note that ρ_{sc} is the total density matrix of the system + oscillators. Tracing out the oscillators, we get the reduced density matrix of the system, i.e.,

$$\rho_s = \text{Tr}_c(\rho_{\text{sc}}). \quad (12)$$

For simplicity, the initial state can be taken as $\rho_{\text{sc}}(0) = \rho_s(0) \otimes \rho_{\text{vac}}^{\otimes M}$, where $\rho_s(0)$ is the initial state of the system and ρ_{vac} is the vacuum state of the harmonic oscillator.

A key problem is determining what kind of non-Markovian environment this pseudomode model can characterize (or what is the COF like of this pseudomode model). In Appendix A, we exactly calculated the expression of the pseudomode's COF, i.e.,

$$C_{\text{pse}}(t) \equiv \langle \hat{B}(t) \hat{B}^\dagger \rangle = \sum_{j=1}^M \lambda_j e^{\gamma_j t}, \quad (13)$$

with $\hat{B}(t) \equiv e^{i\hat{H}_B t} \hat{B} e^{-i\hat{H}_B t}$. Specifically, γ_j are roots of the equation

$$\sum_{l=1}^M \frac{-\frac{1}{2} |\mu_l|^2}{i\Omega_l + \gamma_j} = 1, \quad (14)$$

and

$$\lambda_j = \frac{\sum_{k=1}^M \sum_{l=1}^M \eta_k \eta_l^* Z_{k,j} Z_{l,j} \mu_k \mu_l^*}{\sum_{n=1}^M Z_{n,j}^2 |\mu_n|^2}, \quad (15)$$

where we have defined

$$Z_{n,j} := \frac{1}{i\Omega_n + \gamma_j}. \quad (16)$$

Note that Eq. (14) is an M -order polynomial equation; thus it gives M roots $\gamma_1, \gamma_2, \dots, \gamma_M$. It should be mentioned that we always have $\text{Re}[\gamma_j] < 0$; this is because the COF must decay to 0 when $t \rightarrow \infty$, and hence requires $e^{\gamma_j t} \rightarrow 0$, which is consistent with physical intuition. After knowing those γ_j values, we can directly calculate λ_j by Eq. (15) and hence obtain the analytical expression of $C_{\text{pse}}(t)$ by Eq. (13).

Recalling the local dissipation case [44,48], we have the parameter relation $\frac{-\frac{1}{2} |\mu_l|^2}{i\Omega_l + \gamma_j} = 1$ for all l . But for the collective dissipation case, the parameter relation is given by Eq. (14); i.e., the sum over l is equal to 1, which clearly shows the difference between the two cases. Another difference can be seen from Eq. (15). For the local dissipation case, we always have $\lambda_j = |\eta_j|^2 \geq 0$. But for the collective case, λ_j is usually a complex number, which extends the form of $C_{\text{pse}}(t)$.

IV. DETERMINING THE PSEUDOMODE PARAMETERS

By now we have obtained the expression of the pseudomode's COF, i.e., Eqs. (13)–(16). But the practical issue is that, given an original open quantum system model shown in Fig. 1(a) with a concrete COF, $C(t)$, how does one design a pseudomode model [shown in Fig. 1(d)] equivalent to the original one. The answer is that we need to determine the pseudomode parameters (Ω_j, μ_j, η_j) making $C_{\text{pse}}(t) = \sum_{j=1}^M \lambda_j e^{\gamma_j t} \approx C(t)$, which can be done through three steps.

(i) Given a $C(t)$, we use the Prony method [41,50] (or see Appendix B) to decompose the COF to $C(t) \approx \sum_{j=1}^M \tilde{\lambda}_j e^{\tilde{\gamma}_j t}$. Here, $\tilde{\lambda}_j$ and $\tilde{\gamma}_j$ are usually complex numbers.

(ii) Solving the equation group

$$\sum_{l=1}^M \frac{-\frac{1}{2} |\mu_l|^2}{i\Omega_l + \tilde{\gamma}_j} = 1, \quad \text{with } j = 1, 2, \dots, M, \quad (17)$$

we can easily determine one choice of Ω_j and μ_j . Note that Ω_j is a real number (positive or negative), but μ_j can be a complex number. For the sake of simplicity, we assume that μ_j can also be a real number (positive or negative).

(iii) Replace γ_j by $\tilde{\gamma}_j$ in Eq. (15) and hence directly obtain the expression of $\lambda_j(\eta_1, \eta_2, \dots, \eta_M)$. Finally, solve the equation's group $\lambda_j(\eta_1, \eta_2, \dots, \eta_M) = \tilde{\lambda}_j$, with $j = 1, 2, \dots, M$, which gives the optimal values of $\eta_1, \eta_2, \dots, \eta_M$. Here, those η_j values are usually complex numbers.

After getting all the pseudomode parameters, the original open quantum system can be simulated by solving the Lindblad master equation given by Eq. (9). Tracing out the pseudomode oscillators, we obtain the reduced density matrix of the system, i.e., $\rho_s = \text{Tr}_c(\rho_{sc})$.

V. EXAMPLES: THE SPIN-BOSON MODEL

A. Pure-dephasing spin-boson model

We now consider N 1/2-spin ensemble dissipating in a boson environment with the spin Hamiltonian $\hat{H}_s = \omega_0 \hat{J}_z$, where \hat{J}_z is the total spin- z operator of the spin ensemble. The total Hamiltonian and the interaction Hamiltonian are given by Eqs. (1) and (3) with $\hat{S} = \hat{J}_z$. Given the bath temperature T and the spectral density function $J(\omega) = \sum_k |g_k|^2 \delta(\omega - \omega_k)$, the model can be exactly solved. We expand the Hilbert space by the basis $|m\rangle$, with $m = -j, -j+1, \dots, j-1, j$ and $j \equiv N/2$, where $|m\rangle$ is the common eigenstate of \hat{J}^2 and \hat{J}_z , i.e., $\hat{J}^2|m\rangle = j(j+1)|m\rangle$ and $\hat{J}_z|m\rangle = m|m\rangle$. If we take the initial state $\rho_s(0) = (|j\rangle + |-j\rangle)/\sqrt{2}$, the exact solution of the reduced density matrix is given by

$$\rho_s(t) = \frac{|j\rangle\langle j| + |-j\rangle\langle -j|}{2} + \frac{e^{-N^2\Gamma(t)}}{2} (e^{-iN\omega_0 t} |j\rangle\langle -j| + e^{iN\omega_0 t} |-j\rangle\langle j|), \quad (18)$$

where

$$\Gamma(t) = \int_0^\infty d\omega J(\omega) \coth\left(\frac{\omega}{2K_b T}\right) \frac{1 - \cos(\omega t)}{\omega^2}. \quad (19)$$

As an example, we consider an environment with its spectral density function [40,51]

$$J(\omega) = \begin{cases} \chi \frac{\omega^3}{\pi \omega_c^2} \sqrt{1 - \omega^2/\omega_c^2} & (\text{for } 0 \leq \omega \leq \omega_c), \\ 0 & (\text{for } \omega \geq \omega_c), \end{cases} \quad (20)$$

where χ is the coupling strength and ω_c is the cutoff frequency. For the case of zero temperature, we can calculate

$$\Gamma(t) = \frac{\chi}{2\omega_c t} \text{St}(2, \omega_c t), \quad (21)$$

where $\text{St}(\dots)$ is the Struve function.

To show the three-step process of determining the pseudomode parameters, we start from the two-pseudomode case, with harmonic oscillator frequencies (Ω_1, Ω_2) , dissipation rates (μ_1, μ_2) , and interaction strengths (η_1, η_2) . These parameters can be determined by the three-step method mentioned in the previous section. Specifically, we first use the Prony method to decompose the COF to $C(t) \approx \sum_{j=1}^2 \tilde{\lambda}_j e^{\tilde{\gamma}_j t}$, which gives $(\tilde{\lambda}_1, \tilde{\lambda}_2) = (4.139 + 4.834i, 4.139 - 5.441i)$ and

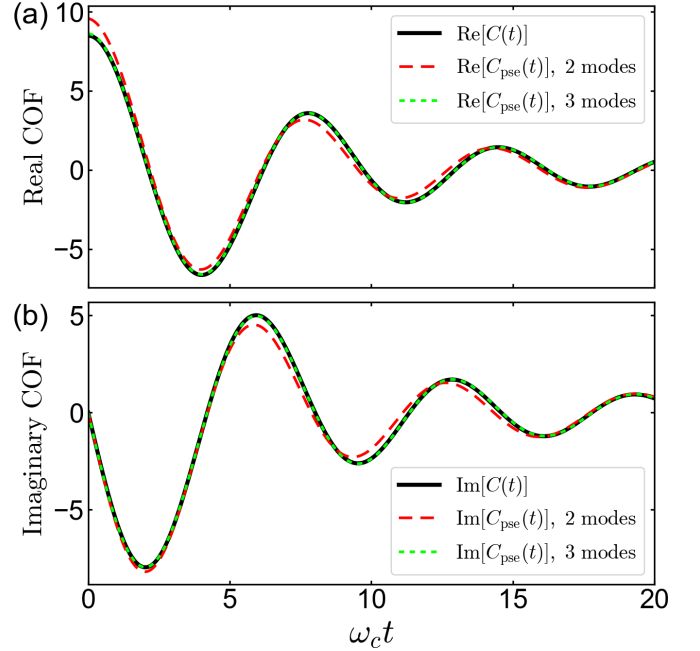


FIG. 2. The real part and the imaginary part of the COF for the original model and the pseudomode model with pseudomode oscillator numbers $M = 2$ and $M = 3$, where the spectral density of the original model is given by Eq. (20). In all figures, we take $\chi = 2$ and $\omega_c = 10$. The pseudomode parameters of the two-mode case: $(\Omega_1, \Omega_2) = (5.151, 9.819)$, $(\mu_1, \mu_2) = (2.161, 1.518)$, and $(\eta_1, \eta_2) = (-0.979 - 2.331i, 0.738 + 1.756i)$. The pseudomode parameters of three-mode case: $(\Omega_1, \Omega_2, \Omega_3) = (2.308, 7.612, 10.234)$, $(\mu_1, \mu_2, \mu_3) = (-2.147, 1.626, 1.574)$, and $(\eta_1, \eta_2, \eta_3) = (0.755, 2.73, -0.764)$.

$(\tilde{\gamma}_1, \tilde{\gamma}_2) = (-0.951 - 9.228i, -2.537 - 5.743i)$, where $C(t)$ is calculated by Eq. (4). Next, solving the equation group

$$\frac{-\frac{1}{2}|\mu_1|^2}{i\Omega_1 + \tilde{\gamma}_j} + \frac{-\frac{1}{2}|\mu_2|^2}{i\Omega_2 + \tilde{\gamma}_j} = 1, \quad \text{with } j = 1, 2, \quad (22)$$

we obtain $(\Omega_1, \Omega_2) = (5.151, 9.819)$ and $(\mu_1, \mu_2) = (2.161, 1.518)$. Note that the solution is nonunique; we only need to choose one solution. Once $\Omega_{1,2}$ and $\mu_{1,2}$ are obtained, we can directly obtain the expression of $\lambda_{1,2}$ by replacing $\gamma_{1,2}$ with $\tilde{\gamma}_{1,2}$ in Eq. (15), i.e., $\lambda_1 = (-0.119 + 0.112i)|\eta_1|^2 - (0.177 + 0.39i)(\eta_1 \eta_2^* + \eta_2 \eta_1^*) + (1.119 - 0.112i)|\eta_2|^2$ and $\lambda_2 = (1.119 - 0.112i)|\eta_1|^2 + (0.177 + 0.39i)(\eta_1 \eta_2^* + \eta_2 \eta_1^*) - (0.119 - 0.112i)|\eta_2|^2$.

Finally, solving $\lambda_{1,2} = \tilde{\lambda}_{1,2}$, which gives the optimal solution $(\eta_1, \eta_2) = (-0.979 - 2.331i, 0.738 + 1.756i)$. In Fig. 2, we compare the original COF $C(t)$ with the pseudomode COF $C_{\text{pse}}(t)$, given by Eqs. (4) and (13), respectively. For the two-mode case, one can find that the pseudomode COF does not perfectly coincide with the original COF. To get a better fitting, we consider three pseudomode oscillators. Using the same procedures mentioned above, we get the pseudomode parameters shown in the caption of Fig. 2. One can find that the pseudomode COF perfectly matches with the original COF for the three-mode case.

After determining those pseudomode parameters, we can describe the time evolution by a Lindblad master equation

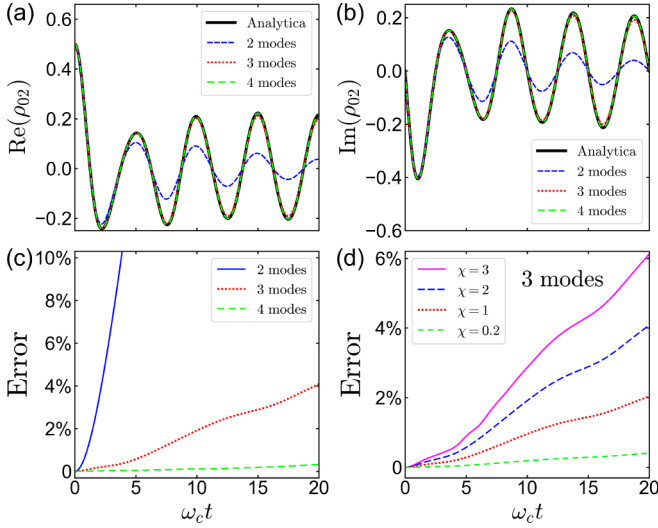


FIG. 3. (a) and (b) The real part and the imaginary part of the density matrix element $\rho_{02} \equiv \langle 1|\rho_s - 1\rangle$ for the analytical result [calculated by Eqs. (18) and (21)] and the pseudomode method's result. (c) and (d) The relative error of ρ_{02} between the analytical result and the pseudomode method's result with different pseudomodes number and coupling strength χ , calculated by Eq. (23). In all figures, we take the spin number $N = 2$ and the spin frequency $\omega_0 = 2\pi$. The pseudomode model parameters of the four-mode case: $(\Omega_1, \Omega_2, \Omega_3, \Omega_4) = (8.608, 10.362, 0.982, 5.198)$, $(\mu_1, \mu_2, \mu_3, \mu_4) = (1.306, 1.609, 1.990, 1.598)$, and $(\eta_1, \eta_2, \eta_3, \eta_4) = (2.045 - 0.992i, -0.386 + 0.166i, 0.192 - 0.036i, -1.554 + 0.837i)$. Other parameters are the same as those in Fig. 2.

given by Eq. (9). Tracing out the pseudomode oscillators, we obtain the reduced density matrix of the spin system, i.e., $\rho_s = \text{Tr}_c(\rho_{sc})$. In Figs. 3(a) and 3(b), we compare the numerical solution of Eq. (9) with the analytical solution by taking different numbers of pseudomode harmonic oscillators. Here we have taken the spin number $N = 2$ and the temperature $T = 0$. One can find that the four-mode case coincides with the exact analytical solution. The relative error between the analytical solution and the numerical solution is defined as

$$\text{Error}(\rho_{\text{ana}}, \rho_{\text{num}}) \equiv \frac{|\rho_{\text{ana}} - \rho_{\text{num}}|}{|\rho_{\text{ana}} + \rho_{\text{num}}|}. \quad (23)$$

As shown in Fig. 3(c), we show the error of $\langle 1|\rho_s| - 1\rangle$. The maximal error is about 4% for the three-mode case and no more than 0.4% for the four-mode case, which verifies the validity of our method.

The accuracy is also affected by the coupling strength. In Fig. 3(d), we show the error with different values of the coupling strength χ , where we have taken three pseudomodes. When the coupling strength χ increases, the accuracy becomes slightly worse. This is because the increase of coupling strength amplifies the mismatch of the COF. If we expect a higher accuracy, we need to increase the number of pseudomode harmonic oscillators. Therefore, the strong-coupling model requires more pseudomodes and more computation resources.

Next, we consider an Ohmic spectral environment with the spectral density function $J(\omega) = \chi \omega e^{-\omega/\omega_c}$ [7], where χ is the coupling strength and ω_c is the cutoff frequency. For the zero

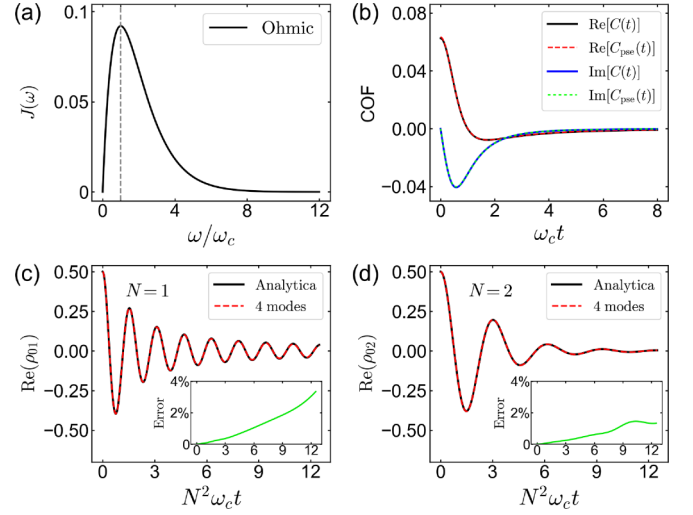


FIG. 4. (a) The spectral density function of the Ohmic spectral environment. (b) The real part and the imaginary part of the COF for the original Ohmic spectral model and the pseudomode model with four pseudomodes. (c) and (d) With spin numbers $N = 1$ and $N = 2$, the real part of the matrix elements $\rho_{01} \equiv \langle \frac{1}{2}|\rho_s| - \frac{1}{2}\rangle$ and $\rho_{02} \equiv \langle 1|\rho_s| - 1\rangle$ for the analytical result [calculated by Eqs. (18) and (24)] and the numerical result [calculated by Eqs. (9)–(12)]. The insets are the relative errors of ρ_{01} and ρ_{02} between the analytical result and the numerical result. In all panels, we take the spin frequency $\omega_0 = 1$, the coupling strength $\chi = 1$, and the cutoff frequency $\omega_c = 0.25$. The pseudomode parameters of the four-mode case: $(\Omega_1, \Omega_2, \Omega_3, \Omega_4) = (0.0389, -0.4886, 0.3681, 1.5722)$, $(\mu_1, \mu_2, \mu_3, \mu_4) = (0.314, 1.117, -0.6121, -1.287)$, and $(\eta_1, \eta_2, \eta_3, \eta_4) = (-0.0597 + 0.0348i, -0.002 - 0.021i, -0.1588 + 0.1569i, 0.0531 - 0.074i)$.

temperature case, $\Gamma(t)$ has the simple form

$$\Gamma(t) = \frac{\chi}{2} \ln(1 + \omega_c^2 t^2). \quad (24)$$

To simulate the time evolution by our pseudomode method, we consider four pseudomodes. The comparison of COFs is plotted in Fig. 4(b), which shows a perfect match. Taking different spin numbers N , we compare the numerical solution of Eq. (9) with the analytical solution in Figs. 4(c) and 4(d). One can find that all the cases indicate a high accuracy.

This pseudomode method is also valid for finite temperature. In Fig. 5, we show the accuracy under the Ohmic spectral environment with the temperature $K_b T = 2.5\omega_c$. One can find that the error can be controlled within 1.3% by two pseudomodes and 0.17% by three pseudomodes.

B. Full spin-boson model

If we consider a more complicated model with the spin Hamiltonian $\hat{H}_s = \omega_0 \hat{J}_z + \omega_\Delta \hat{J}_x$ and the interaction Hamiltonian $\hat{V} = \hat{J}_z \otimes \hat{B}$, the model cannot be analytically solved. But, we can also numerically solve the model by our pseudomode method. We test our method by comparing with the HEOM method under the Ohmic spectral environment. Here, we consider $N = 1$ (i.e., a two-level system) and take the initial state $\rho_s(0) = (|\uparrow\rangle + |\downarrow\rangle)/\sqrt{2}$. The comparisons of $\langle \hat{\sigma}_z \rangle$

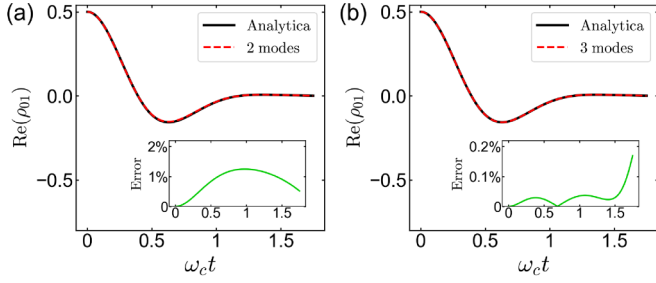


FIG. 5. With the temperature $K_b T = 2.5\omega_c$ and the spin number $N = 1$, the real part of the matrix element $\rho_{01} \equiv \langle \frac{1}{2} | \rho_s - \frac{1}{2} \rangle$ for the analytical result and the numerical result. The insets are relative errors of ρ_{01} . The pseudomode parameters of the two-mode case: $(\Omega_1, \Omega_2) = (-0.3084, 0.7481)$, $(\mu_1, \mu_2) = (0.9277, 1.21)$, and $(\eta_1, \eta_2) = (0.175 - 0.4117i, -0.1441 + 0.3389i)$. The pseudomode parameters of the three-mode case: $(\Omega_1, \Omega_2, \Omega_3) = (-0.0463, 1.0955, -1.3298)$, $(\mu_1, \mu_2, \mu_3) = (0.6022, 1.228, 1.1936)$, and $(\eta_1, \eta_2, \eta_3) = (-0.4859 - 0.2077i, 0.19516 + 0.05i, -0.007094 + 0.04962i)$.

and $\langle \hat{\sigma}_x \rangle$ are shown in Fig. 6, which verifies the validity of our pseudomode method.

C. Spontaneous emission model

We now consider a 1/2-spin dissipating in an Ohmic spectral environment at zero temperature. The total Hamiltonian is given by Eq. (1) with $\hat{H}_s = \frac{\omega_0}{2} \hat{\sigma}_z$. The interaction Hamiltonian with a rotating-wave approximation is given by

$$\hat{V} = \hat{\sigma}_- \otimes \hat{B}^\dagger + \hat{\sigma}_+ \otimes \hat{B}, \quad (25)$$

where $\hat{\sigma}_z$ and $\hat{\sigma}_\pm$ are the Pauli operators and $\hat{B} = \sum_k g_k \hat{b}_k$. For such a rotating-wave approximation interaction Hamiltonian, if we take the initial state $\rho_s(0) = (|\uparrow\rangle + |\downarrow\rangle)/\sqrt{2}$, the reduced density matrix of the spin can be analytically written

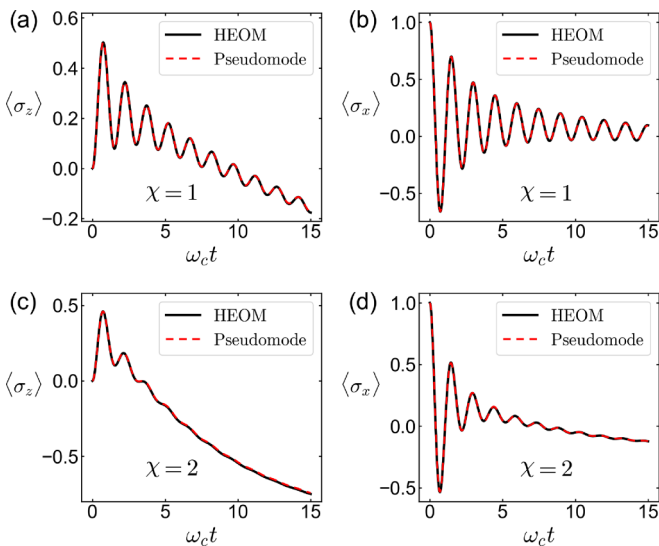


FIG. 6. Numerical result using four pseudomode oscillators vs the HEOM method under the Ohmic spectral environment. We take $\omega_c = 0.25$, $\omega_0 = 1$, $\omega_\Delta = 0.3$, and $T = 0$. The pseudomode model parameters in panels (a) and (b) are the same as those in Fig. 4.

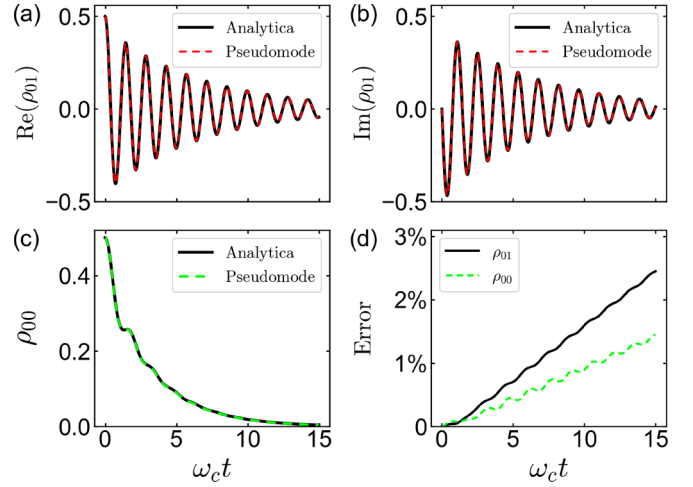


FIG. 7. (a)–(c) The matrix element ρ_{00} and ρ_{01} for the analytical result [calculated by Eqs. (26) and (27)] and the numerical result with four pseudomode oscillators. (d) The relative errors of ρ_{00} and ρ_{01} between the analytical result and the numerical result. The pseudomode model parameters are the same as those in Fig. 4.

as [1,52]

$$\rho_s(t) = \begin{bmatrix} \frac{1}{2} |\alpha(t)|^2 & \frac{1}{2} \alpha(t) \\ \frac{1}{2} \alpha^*(t) & 1 - \frac{1}{2} |\alpha(t)|^2 \end{bmatrix}, \quad (26)$$

where $\alpha(t)$ obeys the equation

$$\dot{\alpha}(t) + i\omega_0 \alpha(t) + \int_0^t C(t-\tau) \alpha(\tau) d\tau = 0, \quad (27)$$

and $C(t)$ is given by Eq. (4) with the temperature $T = 0$. The above equation can be solved by the Laplace transform. The model can also be simulated by our pseudomode method. The time evolution is still described by the Lindblad master equation shown by Eq. (9). Different to the pure dephasing case, the Hamiltonian of the pseudomode model is given by

$$H = \frac{\omega_0}{2} \hat{\sigma}_z + \sum_{j=1}^M \Omega_j \hat{c}_j^\dagger \hat{c}_j + \sum_{j=1}^M (\eta_j \hat{\sigma}_- \hat{c}_j^\dagger + \eta_j^* \hat{\sigma}_+ \hat{c}_j). \quad (28)$$

We test the accuracy under the Ohmic spectral environment. Here, we use four pseudomodes and the parameters are the same as those in Fig. 4. In Figs. 7(a)–7(c), we compare the matrix elements $\rho_{00} \equiv \langle \uparrow | \rho_s | \uparrow \rangle$ and $\rho_{01} \equiv \langle \uparrow | \rho_s | \downarrow \rangle$ for analytical result and numerical result. The relative errors are shown in Fig. 7(d), which demonstrates the validity of our method.

VI. EXTENSION TO COMPLICATED MODEL

Our pseudomode method can also extend to more complicated models. For example, as shown in Fig. 8(a), two systems couple to two uncorrelated non-Markovian baths with different interactions $\hat{S}_1 \otimes \hat{B}_1$ and $\hat{S}_2 \otimes \hat{B}_2$. The total Hamiltonian

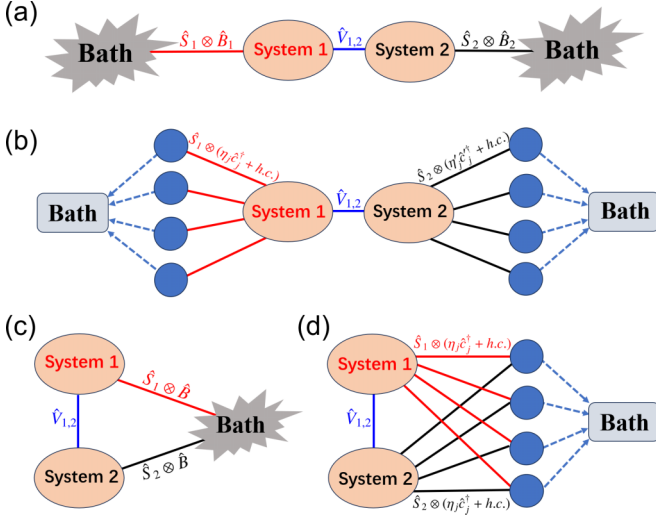


FIG. 8. Pseudomode model to simulate different complicated models. (a) The original OQS in which two systems couple to two different non-Markovian baths. The corresponding pseudomode model is shown in panel (b), which contains two groups of dissipated pseudomode oscillators. (c) The original OQS in which two systems couple to one non-Markovian bath with different interactions. The corresponding pseudomode model is shown in panel (d).

is given by

$$\hat{H}_{\text{tot}} = \hat{H}_s + \hat{H}_{\text{env},1} + \hat{H}_{\text{env},2} + \hat{S}_1 \otimes \hat{B}_1 + \hat{S}_2 \otimes \hat{B}_2, \quad (29)$$

where

$$\hat{H}_s = \hat{H}_{s,1} + \hat{H}_{s,2} + \hat{V}_{1,2}, \quad (30)$$

and $\hat{V}_{1,2}$ denotes the interaction between the two systems. Such a model can be simulated by the corresponding pseudomode model shown in Fig. 8(b). The first original bath is replaced by M_1 dissipated pseudomode oscillators and the second original bath is replaced by M_2 dissipated pseudomode oscillators, with the annihilation operators \hat{c}_j and \hat{c}'_j , respectively. The pseudomode parameters can be determined by matching the corresponding bath COF, which can be done by using the procedures in Sec. IV. After determining those parameters, the evolution is described by

$$\begin{aligned} \frac{\partial \rho_{\text{sc}}}{\partial t} = & -i[\hat{H}, \rho_{\text{sc}}] + \mathcal{D} \left[\sum_{j=1}^{M_1} \mu_j \hat{c}_j \right] \rho_{\text{sc}} \\ & + \mathcal{D} \left[\sum_{j=1}^{M_2} \mu'_j \hat{c}'_j \right] \rho_{\text{sc}}, \end{aligned} \quad (31)$$

where \hat{H} is given by

$$\begin{aligned} \hat{H} = & \hat{H}_s + \sum_{j=1}^{M_1} \Omega_j \hat{c}_j^\dagger \hat{c}_j + \hat{S}_1 \otimes \sum_{j=1}^{M_1} (\eta_j \hat{c}_j^\dagger + \eta_j^* \hat{c}_j) \\ & + \sum_{j=1}^{M_2} \Omega'_j \hat{c}'_j^\dagger \hat{c}'_j + \hat{S}_2 \otimes \sum_{j=1}^{M_2} (\eta'_j \hat{c}'_j^\dagger + \eta'^*_j \hat{c}'_j). \end{aligned} \quad (32)$$

It can be easily extended to larger systems dissipating in L baths with the total Hamiltonian

$$\hat{H}_{\text{tot}} = \hat{H}_s + \sum_{i=1}^L \hat{H}_{\text{env},i} + \sum_{i=1}^L \hat{S}_i \otimes \hat{B}_i. \quad (33)$$

The corresponding pseudomode model's Hamiltonian is

$$\hat{H} = \hat{H}_s + \sum_{i=1}^L \sum_{j=1}^{M_i} [\Omega_{i,j} \hat{c}_{i,j}^\dagger \hat{c}_{i,j} + \hat{S}_i \otimes (\eta_{i,j} \hat{c}_{i,j}^\dagger + \eta_{i,j}^* \hat{c}_{i,j})], \quad (34)$$

where $\hat{c}_{i,j}$ is the annihilation operator of the j th pseudomode oscillator in the i th bath, and M_i is the number of pseudomode oscillators in the i th bath. The model can be solved by

$$\frac{\partial \rho_{\text{sc}}}{\partial t} = -i[\hat{H}, \rho_{\text{sc}}] + \sum_{i=1}^L \mathcal{D} \left[\sum_{j=1}^{M_i} \mu_{i,j} \hat{c}_{i,j} \right] \rho_{\text{sc}}. \quad (35)$$

Similarly, the original model in Fig. 8(c) can also be simulated by the corresponding pseudomode model in Fig. 8(d).

VII. CONCLUSION AND DISCUSSION

In summary, we have proposed a systematic and efficient pseudomode model for simulating open quantum systems under any type of environmental spectrum at any temperature. In our pseudomode model, the system couples to a few pseudomode harmonic oscillators that collectively dissipate in a single Markovian bath. The time evolution is reduced to a Lindblad master equation with only one dissipation part. In principle, any spectral environment can be accurately simulated using our pseudomode model with appropriate parameters. The frequencies and dissipation rates can be determined by a simple equation group. We have tested the accuracy of our model for two exactly solvable spin-boson models: the pure dephasing model and the relaxation model, with two types of spectral environments. We have also considered a more complex spin-boson model and verified our method's validity by comparing it with the HEOM method. Our results consistently exhibit high accuracy. As the number of pseudomode harmonic oscillators increases, the accuracy significantly improves. Generally, taking three or four pseudomode oscillators is sufficient. Our pseudomode method can easily be extended to more complicated and larger systems.

Finally, let us discuss the limitations of the pseudomode method. First, the system and the environment must be initially unentangled. Second, the environment must be describable by a Gaussian bath, usually in the thermal initial state. Finally, the environment operators coupled to the system must be linear, i.e., a linear combination of the creation and annihilation operators of the bosonic degree of freedom. It would be interesting to explore possible generalization of the pseudomode method to go beyond these constraints.

ACKNOWLEDGMENTS

This work was supported by the National Natural Science Foundation of China (Grant No. 12274019), NSAF Joint Fund (Grant No. U2230402), Innovation Program for Quan-

tum Science and Technology (Grant No. 2023ZD0300904). We acknowledge the computational support from the Beijing Computational Science Research Center (CSRC).

APPENDIX A: DERIVATION OF COF

Substituting Eq. (7) into Eq. (13), we have

$$C_{\text{psc}}(t) \equiv \langle \hat{B}(t) \hat{B}^\dagger \rangle = \sum_{j=1}^M \sum_{l=1}^M \eta_j \eta_l^* \langle \hat{c}_j(t) \hat{c}_l^\dagger \rangle, \quad (\text{A1})$$

with $\hat{c}_j(t) \equiv e^{i\hat{H}_B t} \hat{c}_j e^{-i\hat{H}_B t}$ and $\langle \dots \rangle$ denotes expectation at the initial state (vacuum state). To derive the expression of the COF, we need to exactly calculate $\hat{c}_j(t)$ by the Heisenberg motion equations

$$i \frac{d}{dt} \hat{c}_j(t) = \Omega_j \hat{c}_j(t) + \mu_j \sum_k g_k \hat{b}_k(t), \quad (\text{A2})$$

$$i \frac{d}{dt} \hat{b}_k(t) = \omega_k \hat{b}_k(t) + g_k^* \sum_{i=1}^M \mu_i^* \hat{c}_i(t). \quad (\text{A3})$$

Integrating Eq. (A3), we obtain

$$\hat{b}_k(t) = e^{-i\omega_k t} \hat{b}_k - i \sum_{i=1}^M \mu_i^* \int_0^t g_k^* e^{-i\omega_k(t-\tau)} \hat{c}_i(\tau) d\tau. \quad (\text{A4})$$

For convenience, we consider a flat density spectrum, which gives the relation $\sum_k |g_k|^2 e^{-i\omega_k(t-\tau)} = \delta(t-\tau)$, i.e., a Markovian environment. Substituting Eq. (A4) into Eq. (A2), we obtain the differential equation

$$i \frac{d}{dt} \hat{c}_j(t) = \Omega_j \hat{c}_j(t) - i \frac{\mu_j}{2} \sum_{l=1}^M \mu_l^* \hat{c}_l(t) + \mu_j \sum_k g_k e^{-i\omega_k t} \hat{b}_k. \quad (\text{A5})$$

Next, we define $\vec{\hat{c}}(t) \equiv [\hat{c}_1(t), \hat{c}_2(t), \dots, \hat{c}_M(t)]^T$ and $\vec{\hat{s}}(p) \equiv [\hat{s}_1(p), \hat{s}_2(p), \dots, \hat{s}_M(p)]^T$ with $\hat{s}_j(p)$ being the Laplace transform of $\hat{c}_j(t)$. Making the Laplace transform for Eq. (A5), we obtain the relation

$$\vec{\hat{s}}(p) = A^{-1} (\vec{\hat{c}}(0) - \vec{E}), \quad A = \frac{D}{2} + i\Omega + p, \quad (\text{A6})$$

where

$$\vec{E} = [\mu_1, \mu_2, \dots, \mu_M]^T \sum_k \frac{ig_k}{p + i\omega_k} \hat{b}_k, \quad (\text{A7})$$

D is the dissipation coefficient matrix

$$D = \begin{bmatrix} |\mu_1|^2 & \mu_1 \mu_2^* & \cdots & \mu_1 \mu_M^* \\ \mu_2 \mu_1^* & |\mu_2|^2 & \cdots & \mu_2 \mu_M^* \\ \cdots & \cdots & \cdots & \cdots \\ \mu_M \mu_1^* & \mu_M \mu_2^* & \cdots & |\mu_M|^2 \end{bmatrix}, \quad (\text{A8})$$

and $\Omega = \text{diag}[\Omega_1, \Omega_2, \dots, \Omega_M]$ is the frequency matrix. Using the matrix inversion formula, we can calculate the inverse of A , i.e.,

$$A^{-1} = \frac{(i\Omega + p)^{-1}}{h(p)} \left[h(p) \mathcal{I} - \frac{D}{2} (i\Omega + p)^{-1} \right], \quad (\text{A9})$$

where \mathcal{I} is the identity matrix and

$$h(p) = 1 + \frac{1}{2} \sum_{n=1}^M Z_n(p) |\mu_n|^2, \quad (\text{A10})$$

with

$$Z_n(p) = \frac{1}{i\Omega_n + p}. \quad (\text{A11})$$

Using Eqs. (A6) and (A9), we can obtain

$$\hat{s}_j(p) = \frac{Z_j(p)}{h(p)} \left(h(p) \hat{c}_j - \frac{\mu_j}{2} \sum_{i=1}^M Z_i(p) \mu_i^* \hat{c}_i \right) + \sum_k Q_{j,k}(p) \hat{b}_k, \quad (\text{A12})$$

where

$$Q_{j,k}(p) = -\frac{\mu_j Z_j(p)}{h(p)} \frac{ig_k}{p + i\omega_k}. \quad (\text{A13})$$

Making the inverse Laplace transform for $\hat{s}_j(p)$, we obtain the integral form

$$\hat{c}_j(t) = \frac{1}{2\pi i} \int_{\epsilon-i\infty}^{\epsilon+i\infty} \hat{s}_j(p) e^{pt} dp = \frac{1}{2\pi i} \mathcal{I} + \sum_k I_k \hat{b}_k, \quad (\text{A14})$$

where

$$I = \int_{\epsilon-i\infty}^{\epsilon+i\infty} \frac{Z_j(p)}{h(p)} \left(h(p) \hat{c}_j - \frac{\mu_j}{2} \sum_{i=1}^M Z_i(p) \mu_i^* \hat{c}_i \right) e^{pt} dp \quad (\text{A15})$$

and

$$I_k = \frac{1}{2\pi i} \int_{\epsilon-i\infty}^{\epsilon+i\infty} Q_{j,k}(p) e^{pt} dp. \quad (\text{A16})$$

To calculate the integral I , we need to use the residue theorem. First, we should find out the poles, which can be easily realized by solving the equation $h(p) = 0$, i.e.,

$$\sum_{l=1}^M \frac{-\frac{1}{2} |\mu_l|^2}{i\Omega_l + p} = 1, \quad (\text{A17})$$

which gives M poles. If we label the poles as $p = \gamma_k$ ($k = 1, 2, \dots, M$), we arrive at Eq. (14) in the main text. Considering the COF must decay to zero when time $t \rightarrow \infty$, we always have $\text{Re}[\gamma_k] < 0$; i.e., the poles always lie in the left-half plane, which is an inherent physical constraint. In Fig. 9, we plot an infinite semicircle, which helps us to calculate the integral I . According to the residue theorem, we have the relation

$$2\pi i \sum_{k=1}^M \text{res}(\gamma_k) = I + I_c. \quad (\text{A18})$$

According to the Jordan lemma, we have $I_c = 0$; therefore,

$$I = 2\pi i \sum_{k=1}^M \text{res}(\gamma_k). \quad (\text{A19})$$

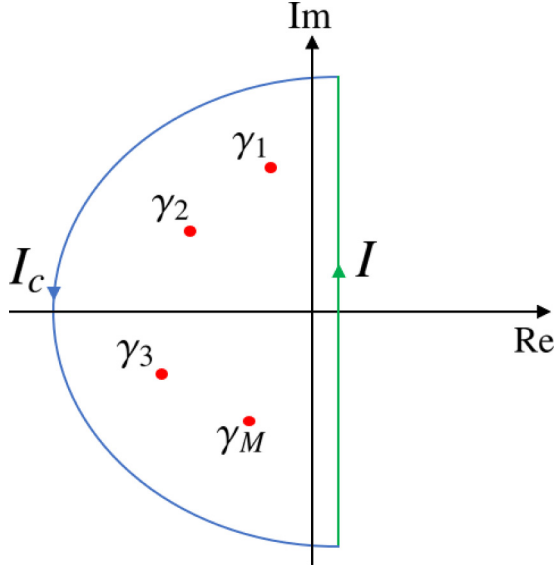


FIG. 9. Calculate the integral at the infinite semicircle using the residue theorem. The red dots are poles γ_k ($k = 1, 2, 3, \dots, M$), which lie in the left-half plane. The circuit integral $I_c + I$ is equal to the sum of residues at each pole. According to the Jordan lemma, the integral I_c is 0.

Next, we need to calculate the residue at each pole:

$$\begin{aligned} \text{res}(\gamma_k) &= \lim_{p \rightarrow \gamma_k} \frac{Z_j(p) \left[h(p) \hat{c}_j - \frac{\mu_j}{2} \sum_{i=1}^M Z_i(p) \mu_i^* \hat{c}_i \right] e^{pt}}{\frac{h(p)}{(p-\gamma_k)}} \\ &= \lim_{p \rightarrow \gamma_k} \frac{Z_j(p) \left[-\frac{1}{2} \mu_j \sum_{i=1}^M Z_i(p) \mu_i^* \hat{c}_i \right] e^{pt}}{-\frac{1}{2} \sum_{n=1}^M Z_n^2(p) |\mu_n|^2} \\ &= \sum_{i=1}^M \xi_{j,i} e^{\gamma_k t} \hat{c}_i, \end{aligned} \quad (\text{A20})$$

where we have defined

$$\xi_{j,i} = \frac{Z_j(\gamma_k) Z_i(\gamma_k) \mu_j \mu_i^*}{\sum_{n=1}^M Z_n^2(\gamma_k) |\mu_n|^2}. \quad (\text{A21})$$

Using Eqs. (A19) and (A14), we have

$$\hat{c}_j(t) = \sum_{k=1}^M \sum_{i=1}^M \xi_{j,i} e^{\gamma_k t} \hat{c}_i + \sum_{k'} I_{k'} \hat{b}_{k'}. \quad (\text{A22})$$

Finally, using Eq. (A1), we obtain the COF of the pseudomode model:

$$\begin{aligned} C_{\text{pse}}(t) &= \sum_{j=1}^M \sum_{l=1}^M \eta_j \eta_l^* \left\langle \sum_{k=1}^M \sum_{i=1}^M \xi_{j,i} e^{\gamma_k t} \hat{c}_i \hat{c}_l^\dagger \right\rangle \\ &= \sum_{j=1}^M \sum_{l=1}^M \eta_j \eta_l^* \left\langle \sum_{k=1}^M \xi_{j,i} e^{\gamma_k t} \hat{c}_i \hat{c}_l^\dagger \right\rangle \\ &= \sum_{k=1}^M \lambda_k e^{\gamma_k t}, \end{aligned} \quad (\text{A23})$$

where

$$\lambda_k = \sum_{j=1}^M \sum_{l=1}^M \eta_j \eta_l^* \xi_{j,l}, \quad (\text{A24})$$

and we have used the fact of $\langle \hat{b}_k \hat{c}_l^\dagger \rangle = 0$. Substituting Eq. (A21) into Eq. (A24), we obtain the equation in the main text:

$$\lambda_k = \frac{\sum_{j=1}^M \sum_{l=1}^M \eta_j \eta_l^* Z_j(\gamma_k) Z_l(\gamma_k) \mu_j \mu_l^*}{\sum_{n=1}^M Z_n^2(\gamma_k) |\mu_n|^2}. \quad (\text{A25})$$

APPENDIX B: DECOMPOSE THE COF BY PRONY METHOD

Given a COF, $C(t)$, one can decompose it to M exponential functions by the Prony method [41,50], e.g., $C(t) \approx \sum_{k=1}^M \tilde{\lambda}_k e^{\tilde{\gamma}_k t}$. Usually, $\tilde{\lambda}_k$ and $\tilde{\gamma}_k$ are complex numbers we need to determine. The procedure contains three steps.

(i) we set a time region $t \in [0, t_{\text{max}}]$ and divide it into $2N$ segments with the segment size $\Delta t = t_{\text{max}}/(2N)$. We label the time points $C(t_n) = C(n\Delta t)$, with $n = 0, 1, 2, \dots, 2N$.

(ii) we construct the Hankel matrix

$$H = \begin{bmatrix} C(t_0) & C(t_1) & \cdots & C(t_{N-1}) & C(t_N) \\ C(t_1) & C(t_2) & \cdots & C(t_N) & C(t_{N+1}) \\ C(t_2) & C(t_3) & \cdots & C(t_{N+1}) & C(t_{N+2}) \\ \vdots & \vdots & \ddots & \vdots & \vdots \\ C(t_N) & C(t_{N+1}) & \cdots & C(t_{2N-2}) & C(t_{2N}) \end{bmatrix}. \quad (\text{B1})$$

Making a singular value decomposition for H , we have

$$H = U^\dagger \Lambda V, \quad (\text{B2})$$

where Λ is a diagonal matrix and U and V are unitary matrices.

(iii) We define R_n as the matrix element of U in the $(M+1)$ th row and the n th column. Solving the eigenvalues of the matrix

$$X = \begin{bmatrix} 0 & 0 & \cdots & 0 & \frac{-R_1}{R_{N+1}} \\ 1 & 0 & \cdots & 0 & \frac{-R_2}{R_{N+1}} \\ 0 & 1 & \cdots & 0 & \frac{-R_3}{R_{N+1}} \\ \vdots & \vdots & \ddots & \vdots & \vdots \\ 0 & 0 & \cdots & 1 & \frac{-R_N}{R_{N+1}} \end{bmatrix}, \quad (\text{B3})$$

we obtain N eigenvalues $x = x_1, x_2, x_3, \dots, x_N$. Picking out all the x_k which satisfies $|x_k| < 1$, we can determine $\tilde{\gamma}_k$ by

$$\tilde{\gamma}_k = \frac{\ln x_k}{\Delta t}, \quad (\text{B4})$$

with $k = 1, 2, \dots, M$.

(iv) Finally, using the least-square method to solve the matrix equation

$$\begin{bmatrix} e^{\tilde{\gamma}_1 t_0} & e^{\tilde{\gamma}_2 t_0} & \cdots & e^{\tilde{\gamma}_M t_0} \\ e^{\tilde{\gamma}_1 t_1} & e^{\tilde{\gamma}_2 t_1} & \cdots & e^{\tilde{\gamma}_M t_1} \\ e^{\tilde{\gamma}_1 t_2} & e^{\tilde{\gamma}_2 t_2} & \cdots & e^{\tilde{\gamma}_M t_2} \\ \vdots & \vdots & \ddots & \vdots \\ e^{\tilde{\gamma}_1 t_{2N}} & e^{\tilde{\gamma}_2 t_{2N}} & \vdots & e^{\tilde{\gamma}_M t_{2N}} \end{bmatrix} \begin{bmatrix} \tilde{\lambda}_1 \\ \tilde{\lambda}_2 \\ \vdots \\ \tilde{\lambda}_M \end{bmatrix} = \begin{bmatrix} C(t_0) \\ C(t_1) \\ C(t_2) \\ \vdots \\ C(t_{2N}) \end{bmatrix}, \quad (\text{B5})$$

we can obtain all $\tilde{\lambda}_k$.

- [1] H.-P. Breuer and F. Petruccione, *The Theory of Open Quantum Systems* (Oxford University, Oxford, 2002).
- [2] I. de Vega and D. Alonso, *Rev. Mod. Phys.* **89**, 015001 (2017).
- [3] V. Gorini, A. Kossakowski, and E. C. G. Sudarshan, *J. Math. Phys.* **17**, 821 (1976).
- [4] G. Lindblad, *Commun. Math. Phys.* **48**, 119 (1976).
- [5] S. Gröblacher, A. Trubarov, N. Prigge, G. D. Cole, M. Aspelmeyer, and J. Eisert, *Nat. Commun.* **6**, 7606 (2015).
- [6] I. de Vega, D. Porras, and J. Ignacio Cirac, *Phys. Rev. Lett.* **101**, 260404 (2008).
- [7] U. Weiss, *Quantum Dissipative Systems* (World Scientific, Singapore, 2012).
- [8] N. Lambert, Y.-N. Chen, Y.-C. Cheng, C.-M. Li, G.-Y. Chen, and F. Nori, *Nat. Phys.* **9**, 10 (2013).
- [9] L. Diósi and W. T. Strunz, *Phys. Lett. A* **235**, 569 (1997).
- [10] L. Diósi, N. Gisin, and W. T. Strunz, *Phys. Rev. A* **58**, 1699 (1998).
- [11] J. Gambetta and H. M. Wiseman, *Phys. Rev. A* **66**, 012108 (2002).
- [12] J. T. Stockburger and H. Grabert, *Phys. Rev. Lett.* **88**, 170407 (2002).
- [13] D. Alonso and I. de Vega, *Phys. Rev. A* **75**, 052108 (2007).
- [14] D. Suess, A. Eisfeld, and W. T. Strunz, *Phys. Rev. Lett.* **113**, 150403 (2014).
- [15] N. Makri, *Chem. Phys. Lett.* **193**, 435 (1992).
- [16] N. Makri, *J. Math. Phys.* **36**, 2430 (1995).
- [17] N. Makri and D. E. Makarov, *J. Chem. Phys.* **102**, 4600 (1995).
- [18] N. Makri and D. E. Makarov, *J. Chem. Phys.* **102**, 4611 (1995).
- [19] R. Egger and C. H. Mak, *Phys. Rev. B* **50**, 15210 (1994).
- [20] J. Prior, A. W. Chin, S. F. Huelga, and M. B. Plenio, *Phys. Rev. Lett.* **105**, 050404 (2010).
- [21] S. R. White, *Phys. Rev. Lett.* **69**, 2863 (1992).
- [22] S. R. White, *Phys. Rep.* **301**, 187 (1998).
- [23] F. Verstraete, J. J. García-Ripoll, and J. I. Cirac, *Phys. Rev. Lett.* **93**, 207204 (2004).
- [24] A. Weichselbaum, F. Verstraete, U. Schollwöck, J. I. Cirac, and J. von Delft, *Phys. Rev. B* **80**, 165117 (2009).
- [25] U. Schollwöck, *Ann. Phys.* **326**, 96 (2011).
- [26] I. de Vega and M.-C. Bañuls, *Phys. Rev. A* **92**, 052116 (2015).
- [27] A. Strathearn, P. Kirton, D. Kilda, J. Keeling, and B. W. Lovett, *Nat. Commun.* **9**, 3322 (2018).
- [28] J. Zhang, Y.-X. Liu, R.-B. Wu, K. Jacobs, and F. Nori, *Phys. Rev. A* **87**, 032117 (2013).
- [29] J. E. Gough, *J. Math. Phys.* **57**, 122101 (2016).
- [30] J. E. Gough, *J. Math. Phys.* **58**, 063517 (2017).
- [31] J. K. Joshua Combes and M. Sarovar, *Adv. Phys.: X* **2**, 784 (2017).
- [32] Y. Tanimura and R. Kubo, *J. Phys. Soc. Jpn.* **58**, 101 (1989).
- [33] Y. Tanimura, *Phys. Rev. A* **41**, 6676 (1990).
- [34] M. Tanaka and Y. Tanimura, *J. Phys. Soc. Jpn.* **78**, 073802 (2009).
- [35] A. Ishizaki and G. R. Fleming, *J. Chem. Phys.* **130**, 234111 (2009).
- [36] A. G. Dijkstra and Y. Tanimura, *Phys. Rev. Lett.* **104**, 250401 (2010).
- [37] Y. Tanimura, *J. Chem. Phys.* **141**, 044114 (2014).
- [38] C. Duan, Q. Wang, Z. Tang, and J. Wu, *J. Chem. Phys.* **147**, 164112 (2017).
- [39] Y. Tanimura, *J. Chem. Phys.* **153**, 020901 (2020).
- [40] T. Ikeda and G. D. Scholes, *J. Chem. Phys.* **152**, 204101 (2020).
- [41] Z.-H. Chen, Y. Wang, X. Zheng, R.-X. Xu, and Y. Yan, *J. Chem. Phys.* **156**, 221102 (2022).
- [42] B. M. Garraway, *Phys. Rev. A* **55**, 2290 (1997).
- [43] E. Arrigoni, M. Knap, and W. von der Linden, *Phys. Rev. Lett.* **110**, 086403 (2013).
- [44] D. Tamascelli, A. Smirne, S. F. Huelga, and M. B. Plenio, *Phys. Rev. Lett.* **120**, 030402 (2018).
- [45] D. Tamascelli, A. Smirne, J. Lim, S. F. Huelga, and M. B. Plenio, *Phys. Rev. Lett.* **123**, 090402 (2019).
- [46] F. Mascherpa, A. Smirne, A. D. Somoza, P. Fernández-Acebal, S. Donadi, D. Tamascelli, S. F. Huelga, and M. B. Plenio, *Phys. Rev. A* **101**, 052108 (2020).
- [47] G. Pleasance, B. M. Garraway, and F. Petruccione, *Phys. Rev. Res.* **2**, 043058 (2020).
- [48] S. Luo, N. Lambert, P. Liang, and M. Cirio, *PRX Quantum* **4**, 030316 (2023).
- [49] N. Lorenzoni, N. Cho, J. Lim, D. Tamascelli, S. F. Huelga, and M. B. Plenio, *Phys. Rev. Lett.* **132**, 100403 (2024).
- [50] G. Beylkin and L. Monzón, *Appl. Comput. Harmonic Anal.* **19**, 17 (2005).
- [51] K. Ando and H. Sumi, *J. Phys. Chem. B* **102**, 10991 (1998).
- [52] Y.-S. Wang, C. Chen, and J.-H. An, *New J. Phys.* **19**, 113019 (2017).